EVALUATING HYDRAULIC AND VEGETATIVE EFFECTS ON RIVER BANK EROSION

Dario Terzic
Advisor: Dr. Karen Prestegaard
GEOL 394
11/25/2019

Abstract

River bank erosion and river migration are related processes. In meandering rivers, bank erosion often drives channel migration and floodplain formation. Bank erosion rates vary among rivers, but river size (e.g. width), power (related to velocity and discharge), shape (width/depth ratio and meander shape), and bank material strength (including plant roots) all affect bank erosion rates. The goal of this research was to monitor bank erosion rates on various time scales, and to measure the hydraulic and bank material parameters that influence bank erosion rates. This was completed by: a) selecting a site near a USGS gauge for which hydraulic data are available, b) obtaining hydraulic and geomorphic data from the USGS gauge data, c) measuring exposed tree roots to monitor long-term bank erosion rates, and d) installing monitoring equipment to determine short term bank erosion rates at various sites along the river where hydraulic and bank material measurements are also obtained.

Introduction and Previous Research

Part 1: Factors that Influence Bank Erosion Rates

Bank erosion is a pertinent topic in both developing and established communities. It is often a defining factor when determining where to build homes, trails, and parks. This is because bank erosion is the driving force behind river migration (Simon et al. 2013). Many researchers in the past have tried to analyze bank erosion rates through various combinations of hydraulic forces and their effects on river width, depth, and velocity (Pizzuto and Mecklenburg 1989, Jerolmack and Mohrig 2007). However, this task has proven difficult; many properties of stream banks and their riparian zones affect the way the river behaves. Properties such as pore water pressure, soil properties such as density or composition, and vegetative properties such as root depth and large woody debris affect bank stability. The factors that affect bank erosion are also affected by the scale of the research and the type of river. Variations in bank erosion rates among reaches of rivers of significantly different sizes have indicated that bank erosion rates increase with river size (e.g. width, discharge; Hooke, 1979). Studies of reaches of river migration with relatively constant discharge but with bends of varying morphology indicate a significant control of meander morphology (e.g. Nanson and Hickin, 1983). Studies of bank erosion along stretches of river in watersheds experiencing changes in discharge due to urbanization or other causes indicate both discharge and local characteristics affect bank erosion rates (e.g. Julian and Torres, 2006, Hooke, 2012). Hooke (2012) used historic (e.g. air photo data) to obtain bank erosion rates in a region with variable discharge. She found that the bank erosion rate for intervals correlated with peak discharge, with one of the main effects being the length of the bank area that eroded per measurements interval. An example of the relationship between discharge and erosion rates is shown in fig. 1.

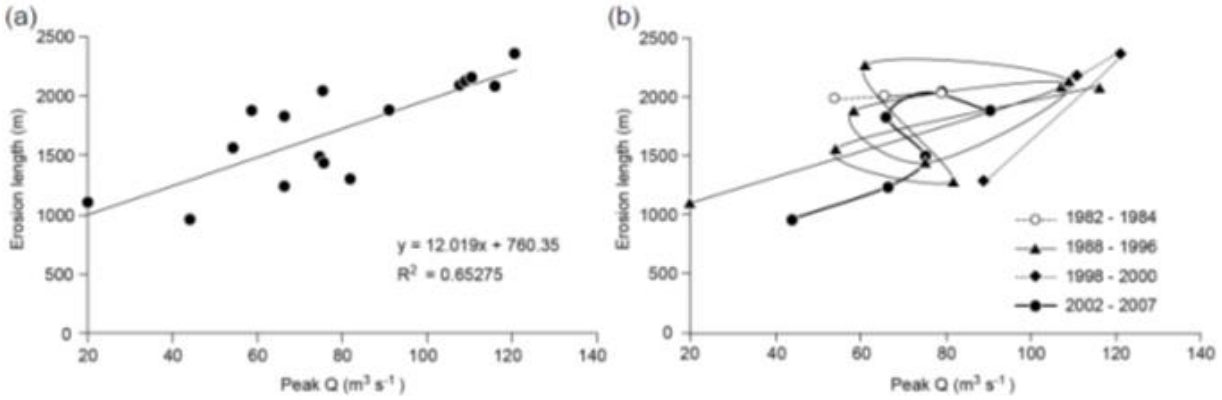

Figure 1. Taken from Hooke 2012 showing the relationship between erosion length and peak discharge.

Part 2: Measurement of Bank Erosion Rates

Many techniques have been used to measure erosion rates, with different techniques used for different time scales, whether or not the river is meandering or braided, and how much vegetation or debris there is in and around the river. A common approach for monitoring long term changes in bank erosion rates is the use of air photo time series as has been done by Hooke (2012). This method is a simple way of understanding the changing migration of a river through time, by taking air photos at multiple time intervals it is easier to see where and when certain places in the river erode more and therefore migrate at a faster rate. This procedure works best for sites where the bank is visible, i.e. in farmlands, grasslands and other locations where trees and other vegetation does not obscure the bank edge from the air. Similarly, direct channel measurements and resurveys are used to monitor erosion rates as well, however, the length of the monitoring period dates to the beginning of measurements. Measurements of this type are made at USGS gauging stations, but these gauges are often located along straight and relatively stable reaches. This process involves taking measurements of bank position and other morphological properties of the bank at sites along a reach of river, these measurements yield erosion rates in specific areas that allows for comparison between sites and therefore evaluation of differences which could increase or decrease erosion rate. Repeat LiDar surveys may also be used to determine channel morphology and its relationship with bank erosion (Pizzuto and Mecklenburg 2009).

Short-term, on the scale of storm events or portions of a year, erosion rates have been monitored by a variety of methods. Bank erosion pins (Leopold and Maddock 1953) have been used in this type of measurement to be able to easily and quickly identify whether a bank is eroding, this is tested by simply inserting a pin or nail into the bank and checking periodically to measure how far the bank has eroded for a specific storm event or to check if it has been washed away due to the eroding bank not being able to hold it in place. This technique has been criticized because the erosion pins could cause local scour and enhance erosion, however, it still appears to be a very effective method with few drawbacks that actively hinder the research process.

In addition to measurements of erosion rates, measurements of bank characteristics that might affect erosion rates can also been conducted. The root depth whether exposed or buried (due to bank erosion or overbank sedimentation respectively) plays an important role in determining the bank erosion in a specific area, the roots size and quantity within a bank work to prevent bank erosion by strengthening the structure of the bank and holding it in place (Pizzuto and Mecklenburg 2009, Malik 2006.).

Figure 2. A photo showing exposed roots along a section of the bank of Seneca Creek

Part 3: Prediction Equations for Bank Erosion Rates

Many researchers have developed predictive equations that can be used to calculate bank erosion rates in rivers. These are largely empirical equations that predict erosion rate as a product of hydraulic effects, vegetative effects, or channel geometry. For example, Julian and Torres (2005) and Randle (2004) evaluated bank erosion rates based on hydraulic characteristics and bank vegetation characteristics. Many other researchers, e.g. Duan (2005), base their predictive equations on stream hydraulic and morphological characteristics. Hickin and Nanson (1983) generated a bank migration equation based on meander bend characteristics. These predictive equations are likely best used for sites with conditions similar to those for which they were developed.

The problem with all of these methods is that these erosion rate predictions may not account for many other river properties that have a significant effect on whether a bank will erode, therefore causing any erosion rate calculated to only be useful for one river or even one site in one river.

There are several predictive equations that include many parameters that vary along a river or among rivers. An example of this type of equation is that by Randle (2004), which expresses erosion rate as a function of factors that increase erosion rates (meander bend characteristics, velocity) and decrease erosion rates by affecting local bank strength (rooting density, morphology, woody debris, etc.).

$$Be = \left\{\left[a1Cs\left(\frac{Wb}{Rc}\right)\right] - \left[a2\left(Ry * \frac{Rd}{Hb}\right) + a3\left(LWD * \frac{dw}{D}\right) + a4(PI) + a5\left(dc * \frac{Hb}{D}\right)\right]\right\} a6 * V$$

Equation 1.

where Be = bank erosion rate, Cs = bed sediment concentration, Wb = bankfull channel width, Rc = channel radius of curvature, Ry = fraction of bank covered by vegetation roots, Rd = vegetation root depth, Hb = bank height, LWD = fraction of bank covered by tree of large woody debris, Dw = average height of large woody debris jams, D = hydraulic depth of channel, PI = plastic index, Dc = portion of bank sediment too coarse for incipient motion, V = mean channel velocity [L/T], and a1 and a6 are empirical coefficients and a2, a3, a4, and a5 are weighting factors.

In the scope of my research I used this bank erosion equation as a guide to the factors that might influence bank erosion rates at my study site. The Randle bank erosion rate equation incorporates many of the river characteristics that have been previously shown to influence bank erosion that are consistent with the characteristics of the study site. These characteristics include river velocity, bend morphology, channel depth, width, rooting depth, root density, and amount/size of woody debris covering banks. I have also measured spatial variations in long-term erosion rates by analyzing short-term erosion rates by making repeated measurements along the channel bank.

Hypothesis

1) The increase in annual peak discharge at the USGS gauge on Seneca Creek is associated with significant channel widening (bank erosion) for the period 1938 to 2018.
2) Bank erosion rates measured from air photos (decadal time scales) increase with (Rc/w) ratio; they are highest on the outside of bends, where velocities are the highest.
3) Short-term erosion rates (measured after flood events) are highest during hydrographs that generated high velocities (and excess shear stress).
4) In the selected study reach rooting depths and bank vegetation protect the bank from erosion and therefore are inversely correlated with local bank erosion rates measured by air photos or erosion pins.

These hypotheses were developed by building off the previous research to suggest that bank erosion rate is affected by hydraulic effects (water velocity, river width, river discharge) in the

long term and throughout the entire river. Local variations in bank erosion rate along a reach of river within shorter time periods is due to heterogeneities of vegetation or rooting depth. The idea behind this is that the hydraulic effects act as an amplifier or reducer to the overall erosion rate of the river while vegetative effects along a reach of river act as buffer between the bank and the water to reduce the rate of erosion in specific areas. As a result, what would occur is that along a reach of river there are varying rates of erosion that can be monitored with different techniques and predicted from measuring the properties of the river at specific sites along said reach.

Study Site and Methods

The study site is a section of Seneca Creek near Dawsonville, Maryland (fig. 3). The site is located upstream of a USGS gauging station. The Seneca Creek watershed contains rapidly suburbanizing areas in Rockville and Gaithersburg, Maryland. As a result, peak discharges in the watershed have been increasing over the past few decades (fig. 4). Examination of the field site indicates high rates of bank erosion (exposed roots, fallen trees, etc.) as well as overbank deposition of coarse sand. During the observation period, I monitored bank erosion that undermined the root structure of a tree (fig 9), which suggests that bank erosion is an active process as whole in this river and specifically in the chosen study area.

Figure 3. An air-photo of the study area along Seneca Creek. The superimposed yellow bar represents 100 meters length, the superimposed white arrow represents north direction. The superimposed circle shows the radius of curvature for one of the meander bends.

Part 1: Temporal Variations in Discharge and Channel Morphology through USGS Gauge Data

USGS Hydraulic Data

Hydraulic data, consisting of river width and depth, velocity, and discharge is available for the period from 1938 to the present. In addition to the peak discharge data, stream measurement data was also be acquired. These data was divided into 10-year increments and used to determine annual average peak discharge, and maximum peak discharge. This approach is similar to the approach taken by Hooke (2009), who used gauge data to obtain average flood discharge values for time increments for which she obtained channel change data.

Air photos of Seneca Creek show the general trace of the channel banks, but the actual bank edge is often covered by trees (fig. 3). Therefore, in addition to the annual peak discharge data, the USGS stream measurement data was used to obtain bankfull channel morphology and velocity data by evaluating the at-a-station hydraulic geometry for each 10-year period. The hydraulic geometry relationships are the power function relationships between discharge and width, depth and velocity at a given station (Leopold and Maddock, 1953). The at-a-station hydraulic geometry equations refer to in-bank flows:

$W = aQ^b$, $D = cQ^f$, $V = kQ^m$
where Q = discharge, w = channel surface width, D = average depth (Area/W), and V = average velocity. Due to continuity, W*D*V = Q; therefore b+f+m = 1.0 and a*c*k = 1.0
An example of Hydraulic Geometry relationships for the time period 1949-1958 is shown in figure 5.

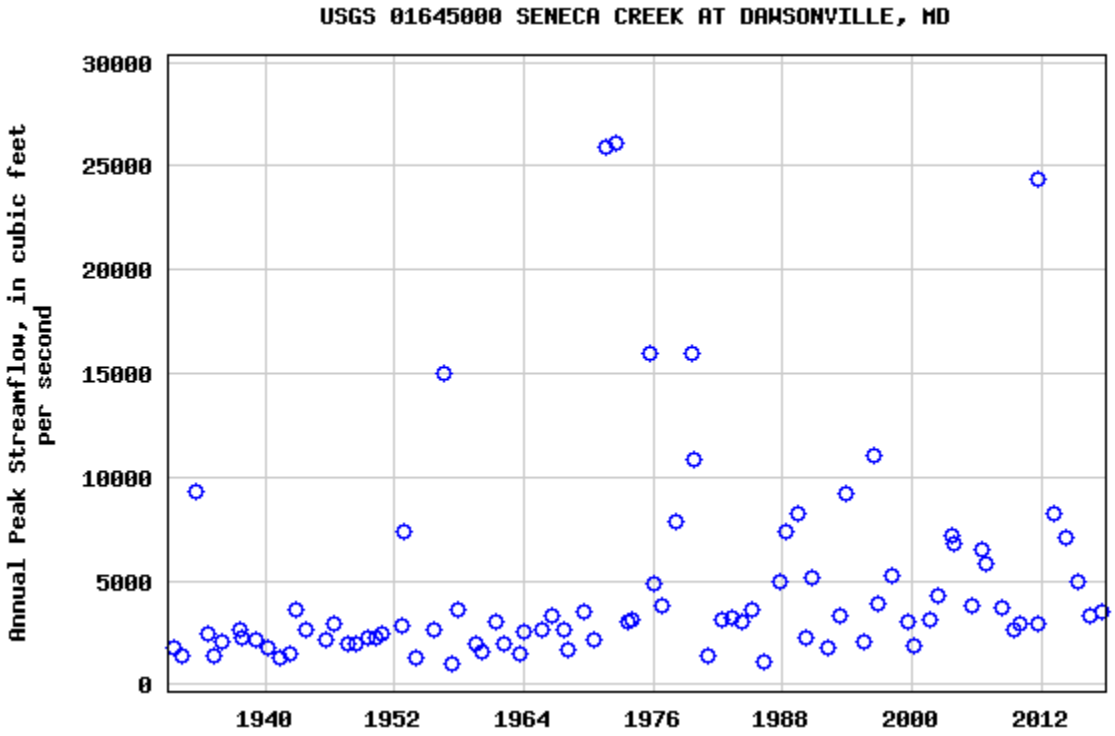

Figure 4. The annual peak discharge through time, shown increasing from 1930 to the present (USGS 2019).

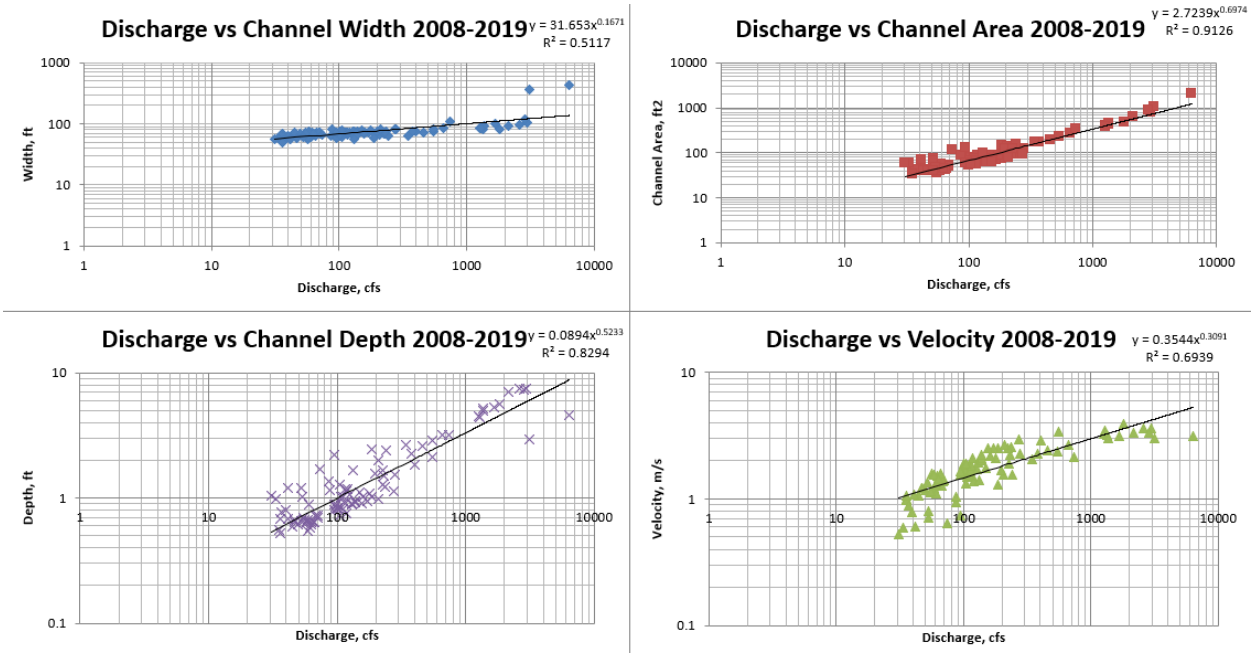

Figure 5. These graphs are an example of the hydraulic geometry relationships taken from USGS gauge data for the years 1949 to 1958.). Bankfull discharge can be identified most clearly on the width versus discharge diagram, which indicates a large increase in width (from 165 feet to 540 feet) for a small change in discharge (1800 to 2,000 cfs) as the channel overtops its bank and uses the floodplain to carry part of the discharge.

The width for the mean annual peak Q was calculated from these hydraulic geometry relationships for each time interval. Similarly, the hydraulic geometry data was used to calculate the discharge, width, depth, and velocity for bankfull flows in each 10-year period (see table 1). Bankfull discharge is commonly the 1.5 year R.I. (Recurrence Interval) discharge, so it will likely be lower than the average annual peak discharge in each time interval.

Table 1: Discharge Data for time intervals

Interval	Ave Annual Peak Discharge, Q, cfs	Maximum Q, cfs	Bankfull Q, cfs ~1.5-year RI	Velocity for Bankfull Q
1939 – 1948	2062	3620	1810	3.05
1949 – 1958	2838	15000	503	3.75
1959 – 1968	2167	3070	373	3.25
1969 - 1978	7805	26100	228	2.09
1979 - 1988	4647	16000	310	2.77
1989 - 1998	4571	11000	209	1.82
1999 - 2008	4329	7130	3610	4.13
2009 - 2018	4448	24400	3120	2.99

In summary, from these USGS hydraulic data, the following information for the 10-year increments has been obtained: average annual peak, Maximum peak Q, and the bankfull characteristics, and the associated bankfull width, depth, and velocity. These data could be used in bank erosion rate predictive equations, which often incorporate discharge and velocity.

Analysis of change and association with discharge

I have evaluated the changes in bankfull channel characteristics at the USGS gauge by determining the bankfull characteristics of each time interval and using these data to determine channel changes between each 10 –year interval. Channel widening is bank erosion, which would be indicated by a positive Δwidth/year. Similarly, an increase in depth would be a positive change in channel depth as Δdepth/year.

Hooke (2012) found a simple relationship between annual bank erosion rate and maximum discharge:

$$E_{mean} = 0.0054 Q_{max}$$

I examined the hydraulic and channel change data to determine whether similarly simple relationships between channel width enlargement rate (bank erosion rate) and discharge exist. It is also possible that the channel will enlarge due to increases in channel depth (due to overbank sedimentation, channel incision, or both) rather than increases in channel width.

Part 2: Spatial Variation in Channel Morphology through Long-term and Short-term Bank Erosion Measurements.

The first part of my study used USGS gauging station data. These data extend over a significant period of time, but only provide information about one cross section of the river. In this part of my study, I examined spatial differences in bank erosion rates, and associated variations in channel morphology and bank characteristics. For this part of my study, I have selected 8 areas along of a reach of Seneca Creek (fig. 6).

Figure 6. Air photo of the study area displaying where specific sites for measurements are located. The superimposed white bar represents 100 meters on the ground and the white arrow is north direction.

These reaches of river were selected to provide a range of planform morphology ranging from tight meander bends (Rc of 20.12 m) to open meander bends (Rc of 29.67 m) to straight reaches (table 2). For these selected reaches, migration rate was estimated by measuring the changes in channel area for each segment divided by the segment length for the 4/2008 and 4/2018 air photos (which were the best resolution and taken during dormant periods for vegetation). These migration amounts were divided by the time interval (10 years) to obtain migration rate. Examples of channel changes between the 2008 and 2018 channels on the air photos are shown in fig. 7.

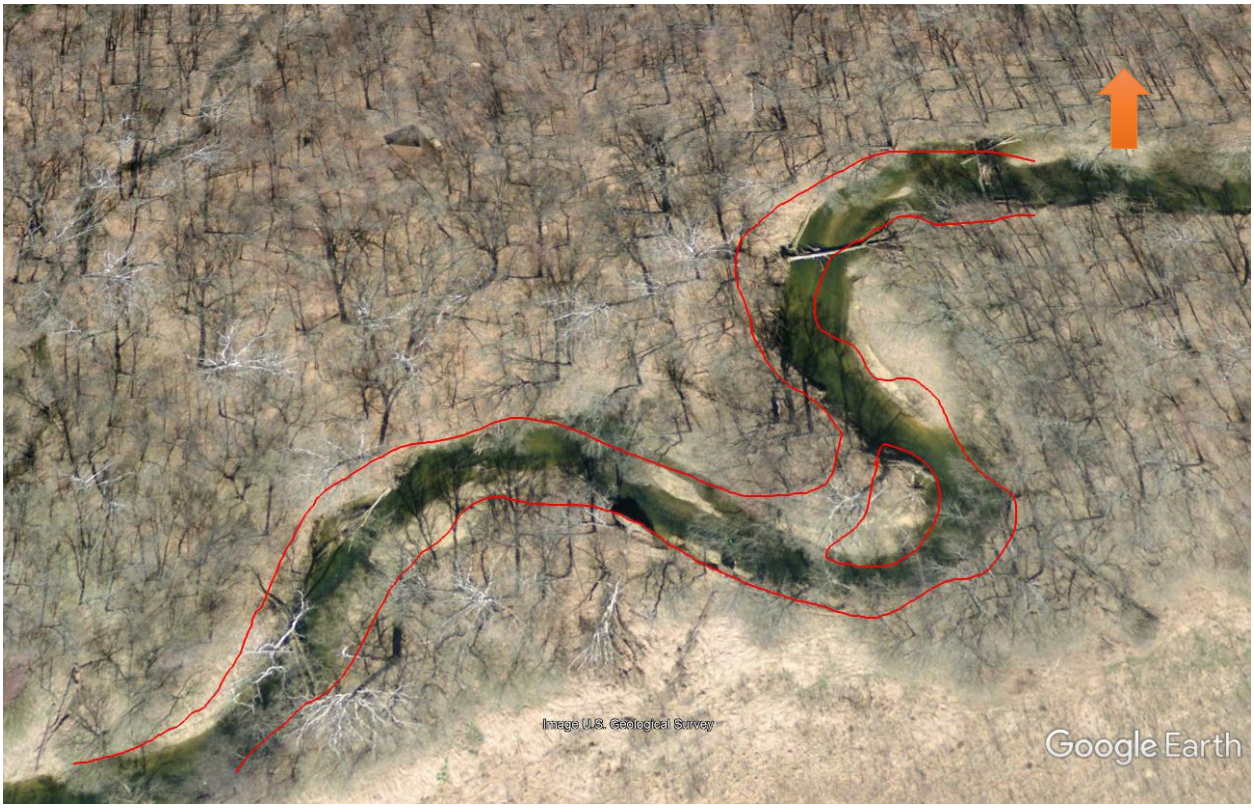

Fig. 7: Channel Boundaries from the 4/2008 channel shown on the 4/2018 image (drawn in Google Earth, the image is from the USGS for both years, the orange arrow is north direction). Note the cut-off chute that was formed and subsequently reconnected in the middle of the bank.

Table 2: Physical Characteristics of the channel of study reaches and associated migration rates

Site Name	**Length (m)**	**Ave Width, m***	**Depth m**	**Rc, m**	**Rc/w**	**Rooting Depth, m**	**Migration Rate, m/yr**
Site 1	70	22.5	1.83	26.08	1.06	1.52	0.03
Site 2	143	13.2	1.8	24.22	2.15	.76	0.93
Site 3	110	13.0	2.13	NA	NA	1.22	0.10
Site 4	52	14.7	2.13	NA	NA	1.07	0.30
Site 5	64	12.15	2.44	20.12	2.65	1.83	0.30
Site 6	113	16.2	2.44	27.4	2.26	0.91	0.05
Site 7	89	10.3	1.83	22.78	1.64	.76	0.92
Site 8	109	18.5	1.83	29.67	1.71	.76	0.20

*Average width = Channel surface area/length; **Average migration rates from 2008 and 2018 air photos calculated as surface area change per unit length divided by time interval.

Short-Term Bank Erosion and Overbank Sedimentation Rates

The 2016 and 2018 air photos indicate that large amounts of woody debris entered the channel after 2016. This debris may have an impact on the amount and location of future bank erosion rates. Therefore, the last set of data that I have collected throughout the year is the actual bank migration through short intervals of time. This was measured through the year after major storm events. These measurements were made at installations near the bank. The process for this was inserting erosion pins flush with the bank at each station along the river (figure 6.) to monitor bank erosion. After storm events the bank will erode inward, leaving the pin behind as a record of where the bank used to be thus yielding erosion data; an example of this method is shown in figure 8.

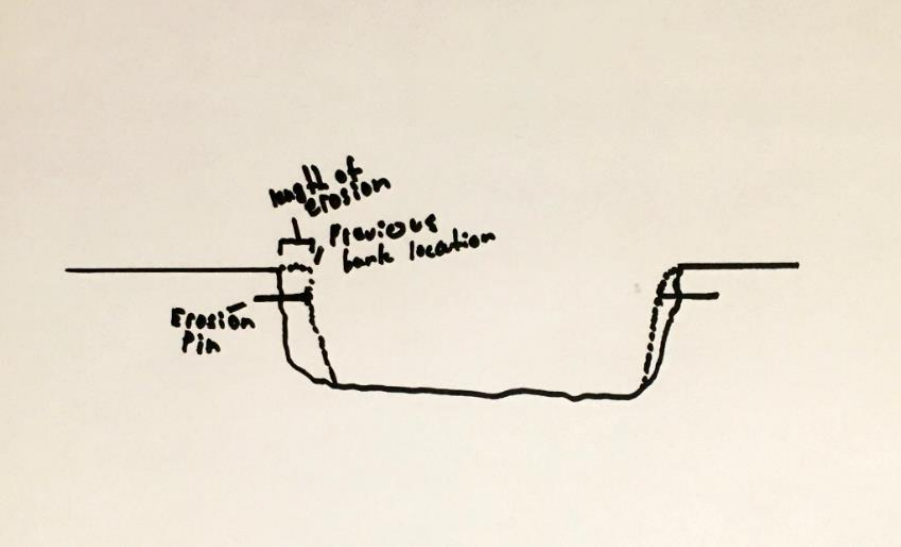

Figure 8. A diagram of the aforementioned erosion pin method.

I have taken reliable measurements on the bank migration and other parameters (such as large river discharge and rooting depths) throughout the year. Throughout the year I have visited the study area many times and there were noticeable changes in the properties along the bank each time. These properties include overhanging banks, exposed roots, fallen trees and slumped banks. These examples of changing river morphology and spatial variations in vegetation all indicate that the river is actively eroding. The error associated with these measurements arise from innate uncertainty in measuring tools i.e. tape measures, google earth satellite accuracy, USGS gauge sites. The percent error in google earth polygon and line measurements is 3.54% and 0.44% respectively (Nogueira and Lopes 2011). The USGS gauge data is accurate to 2%-5%. The tape measure that I am using is accurate to $\pm$ 0.1cm.

Figure 9. A set of photos showing a tree that had fallen within at least a week of observation.

Figure 10. A photo showing the exposed root systems of a tree that had been growing on a bank that has since eroded inland.

Results

Temporal Data

Table 2 shows the physical characteristics of the channel in the study reach. The width of the study reach did not vary significantly but the radius of curvature did. I measured the radius of curvature for each bend five times to obtain errors for each site, table 4 shows this the results below.

Table 4: Physical Characteristics of the channel of study reaches and associated migration rates

Site Name	Length (m)	Ave Width, m*	Depth m	Rc, m	Rc/w	Rooting Depth, m	Migration Rate, m/yr
Site 1	70	22.5	1.83	26.08	1.06	1.52	0.03
Site 2	143	13.2	1.8	24.22	2.15	.76	0.93
Site 3	110	13.0	2.13	NA	NA	1.22	0.10
Site 4	52	14.7	2.13	NA	NA	1.07	0.30
Site 5	64	12.15	2.44	20.12	2.65	1.83	0.30
Site 6	113	16.2	2.44	27.4	2.26	0.91	0.05
Site 7	89	10.3	1.83	22.78	1.64	.76	0.92
Site 8	109	18.5	1.83	29.67	1.71	.76	0.20

*Average width = Channel surface area/length; **Average migration rates from 2008 and 2018 air photos calculated as surface area change per unit length divided by time interval.

Table 5. The average and standard deviation of radius of curvature measurements.

Rc Measurements	site 1	site 2	site 3	site 4	site 5	site 6	site 7	site 8
	25.52	26.12	NA	NA	18.99	27.72	25.82	30.98
	25.73	27.19	NA	NA	21.1	26.22	26.54	29.27
	27.55	22.96	NA	NA	19	28.39	25.51	28.8
	25.26	23.15	NA	NA	19.62	27.52	24.07	29.14
	26.34	24.19	NA	NA	21.87	27.15	22.78	30.17
Avg	26.08	24.722	NA	NA	20.116	27.4	24.944	29.672
St. Dev.	0.91337287	1.864422162	NA	NA	1.304235	0.798718	1.506795	0.889365

The hydraulic geometry equations were used to calculate the peak velocity for the maximum discharge for each time interval, specifically, the discharge versus velocity graph. Doing this allowed showed that intervals with high discharges exhibit higher velocities and as a result greater rates of erosion for the time interval. Table 5 shows the erosion pin data and their association with velocity and discharge.

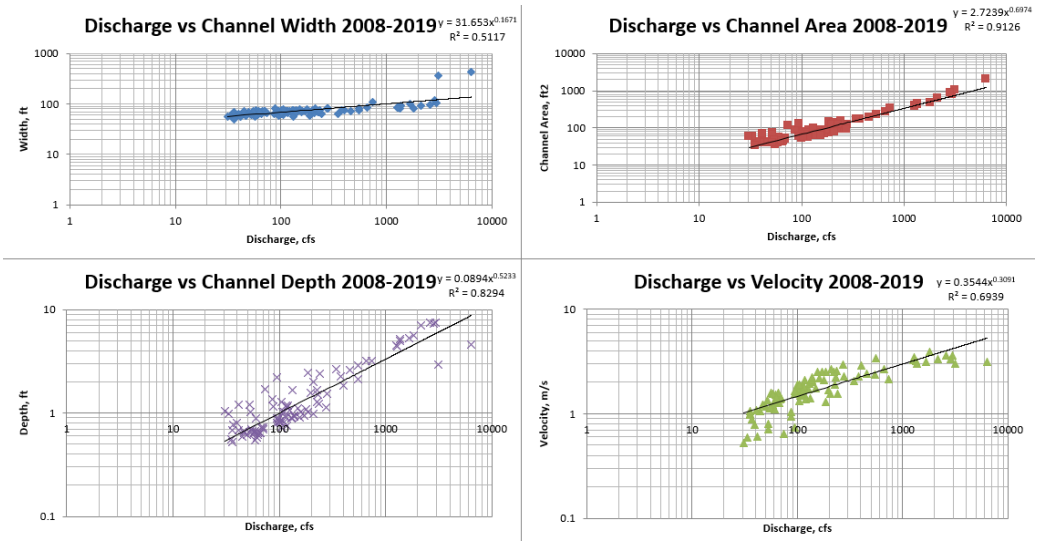

Figure 11. These graphs are an example of the hydraulic geometry relationships taken from USGS gauge data for the years 2008 to 2019.). Bankfull discharge can be identified most clearly on the width versus discharge diagram, which indicates a large increase in width (from 165 feet to 540 feet) for a small change in discharge (1800 to 2,000 cfs) as the channel overtops its bank and uses the floodplain to carry part of the discharge.

Erosion Pin Data (Short Term Event Data)

Erosion pin data was collected over five time intervals from August to November. Figure 12 shows the associated discharges for each of these events and table 5 displays the erosion pin data for each of these time intervals.

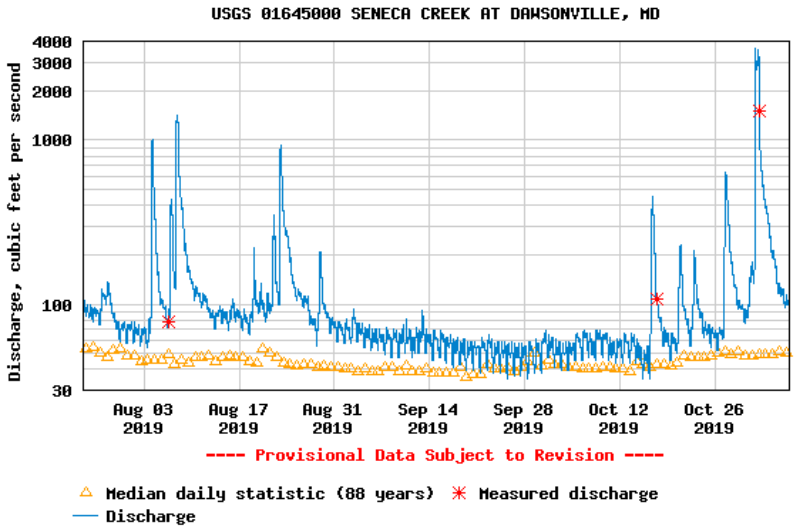

Figure 12. The Discharge hydrograph for the period of July 25th to November 5th during which time the erosion pin data were collected.

Below are the erosion pin data for the five time intervals over which I measured erosion and the associated discharge and velocity values. The erosion data for each time interval shows that the erosion is approximately 1 cm or more, the relationship between peak velocity and erosion is shown in figure 13.

Table 5. Showing the erosion pin data with associated discharge and velocity values.

Avg Root Depth (cm)	7/27-7/30 erosion, cm	8/4-8/6 erosion, cm	8/19-8/21 erosion, cm	9/4-9/5 erosion, cm	10/20-10/22 erosion, cm	10/29-10/31 erosion, cm
91.44	2.54	2.54	30.48	0.762	0.254	12
91.44	0.254	2.794	2.54	2.794	1.016	12
60.96	0.508	0.508	0.254	0.635	0.508	0.508
91.44	1.016	0.762	0.762	0.762	0.762	1.27
91.44	0.508	0.508	1.016	0.762	0.508	0.762
91.44	0.254	1.27	1.27	0.508	1.27	2.54
91.44	0.254	0.762	0.254	0.508	0.254	0.508
91.44	0.254	2.54	2.413	1.27	1.524	0.508
121.92	0.762	3.048	2.54	1.27	12	1.016
152.4	2.54	2.54	2.159	2.54	1.778	1.524
152.4	1.016	1.27	0.762	1.016	0.254	1.016
60.96	0.508	20.32	0.254	0.254	0.508	0.508
91.44	0.254	0.762	2.159	0.508	0.762	0.762
91.44	1.27	1.27	1.016	2.032	0.762	0.762
121.92	0.762	1.27	1.27	1.016	1.016	12
121.92	3.048	2.54	2.794	2.286	1.778	1.016
121.92	0.254	1.27	0.254	0.254	0.508	21.59
91.44	1.27	1.016	0	1.016	0.762	0.508
Erosion Average	1.0	2.6	2.9	1.1	1.5	3.9
Erosion St. Dev.	0.9	4.4	6.8	0.8	2.7	6.2
Peak Discharge, cfs	126	1010	255	93.3	213	457
Peak Velocity, m/s	1.6	3.0	2.0	1.4	1.9	2.4

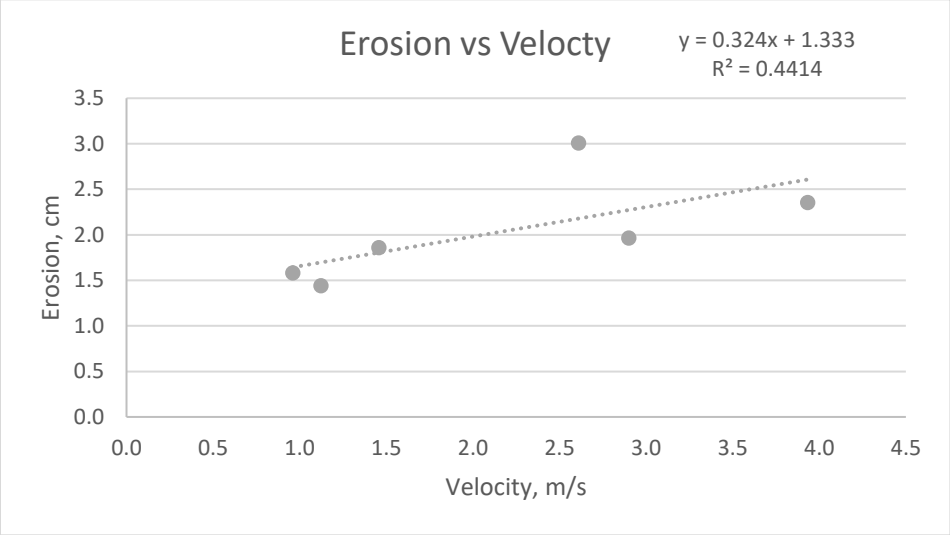

Figure 13. Showing the relationship between velocity and amount of erosion.

Spatial Variation in Erosion Rates From 2008 to 2018 Air Photo Data

Table 2 shows significant variations in erosion rates among the eight channel reaches. This section will examine the erosion rates to the characteristics of each of the reaches. The first figure below shows migration rate versus rooting depth, the second figure below shows the migration rate versus radius of curvature to width ratio.

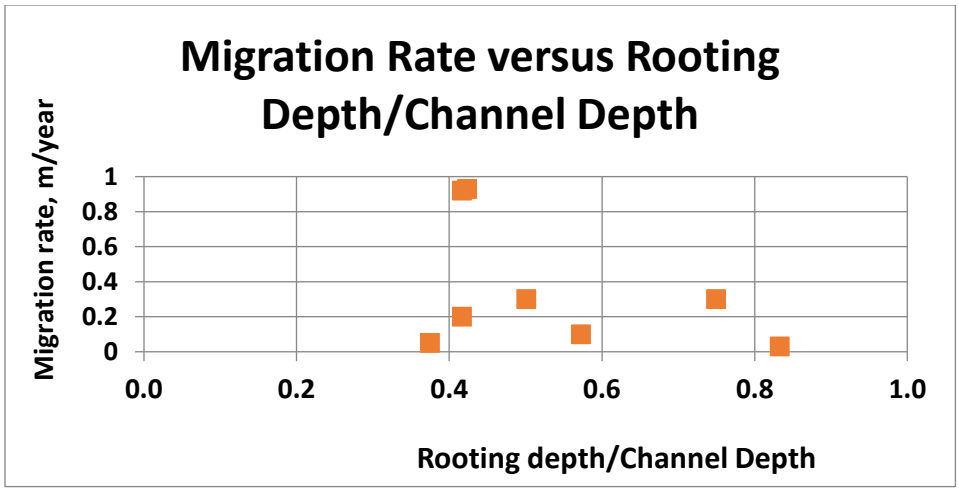

Figure 14. Shows the relationship between migration rate and rooting depths at each site.

Figure 15. Showing the exposed roots of a tree and the eroded bank behind it.

There is a variation in migration rate at each site. While most sites have low migration rate across rooting depths there are several sites where migration rate is high at low rooting depths. This suggests that rooting depth by itself was not a major control on migration rates.

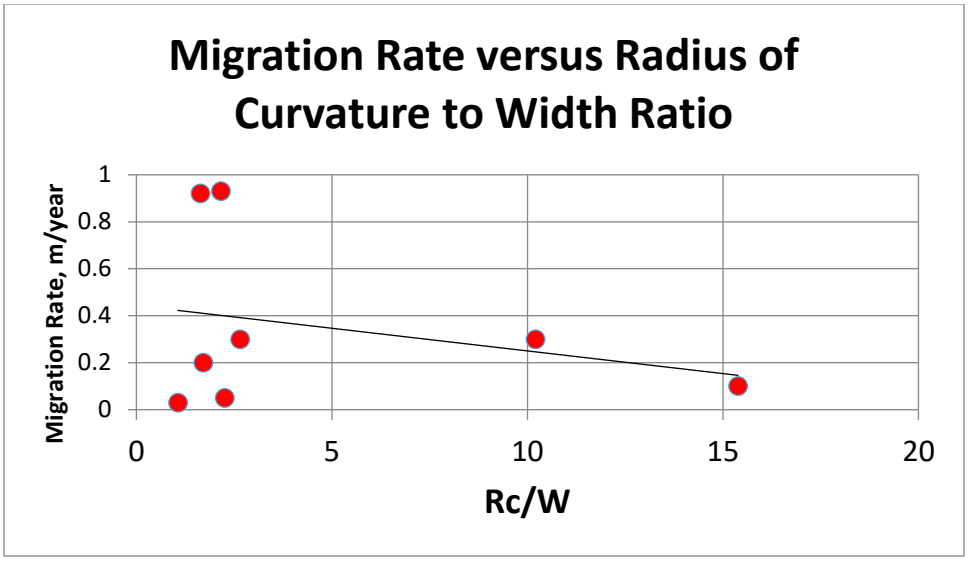

Figure 16. Shows migration rate versus radius of curvature to width ratios.

The highest migration rates were found to be around radius of curvature to widths of about 2.3.

Discussion and Conclusion

Using the Randle equation as a guide I evaluated the importance of the parameters associated with erosion rate. Many of the parameters were found not to be very useful within a reach, rather than among reaches. Some of these parameters were: Rooting depth, large woody debris, the height of debris jams, and bed sediment concentration. This is because the banks of the study reach had a consistent sediment make-up of clay/silt along the lower half to a coarse sand on top that were consistent throughout the reach. The debris did not have an effect on the erosion rates because there was either no large woody debris present or the velocities were high enough to wash them away. Rooting depth was found not to be strongly correlated with erosion rate as stated above since we see that migration rates vary significantly across varying rooting depths. What I did find was that velocity and radius of curvature are more important within this reach, both were observed to affect the erosion rates significantly as shown above. Velocity increases erosion rate and during the study there were multiple storm time intervals that exhibited different velocities with their individual erosion amounts varying as well (Table 3.), velocity has been increasing in this area through time due to urbanization. The radius of curvature to width ratio was also found to be an important factor that controls erosion rate. This is similar to the findings of Hicken and Nanson (1983), in which they found that radius of curvatures from 2 to 3 had the highest migration rates, which is also similar to what is shown in figure 14. Observationally there were many mass wasting events in which the bank slid into the

river as it was undercut by high velocity water, these events usually happened in bends and were seen mostly after larger storms (figure 17).

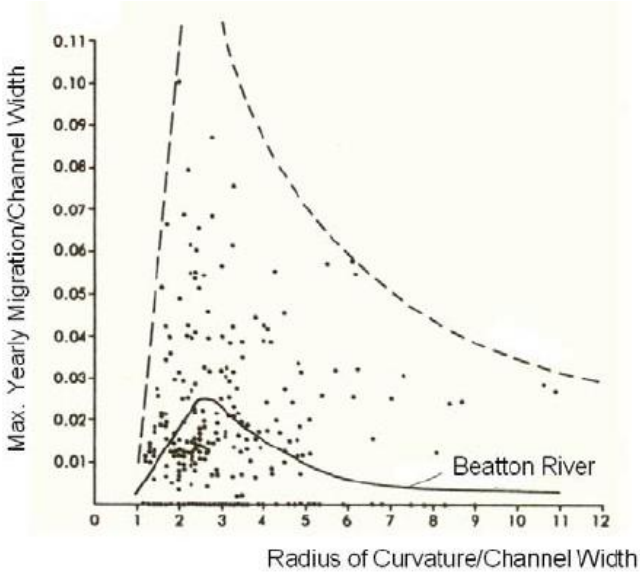

Figure 16. Showing the Migration rate versus radius of curvature to width distribution from Hicken and Nanson 1983.

Figure 17. Showing a mass wasting event in which a section of bank slid into the river.

Bibliography

Duan, J.G., (2005), Analytical Approach to Calculate Rate of Bank Erosion: Journal of Hydraulic Engineering, v. 131, p. 980–990, doi: 10.1061/(asce)0733-9429(2005)131:11(980).

Edésio, Msc & Elias Lopes, Edésio & Ruth, Dra & Nogueira, Ruth. (2011). Proposta Metodológica para Validação de Imagens de Alta Resolução do Google Earth para a Produção de Mapas.

Hooke, J. (2012). Dynamics of bank erosion on the River Dane, England. IAHS-AISH Publication. 356. 57-64.

Hooke, J., (1979), An analysis of the processes of river bank erosion: Journal of Hydrology, v. 42, p. 39–62, doi: 10.1016/0022-1694(79)90005-2.

Jerolmack, D.J., and Mohrig, D., (2007), Conditions for branching in depositional rivers: Geology, v. 35, p. 463, doi: 10.1130/g23308a.1.

Julian, J.P., and Torres, R., (2006), Hydraulic erosion of cohesive riverbanks: Geomorphology, v. 76, p. 193–206, doi: 10.1016/j.geomorph.2005.11.003.

Leopold, L.B., and Maddock, T., (1953), The hydraulic geometry of stream channels and some physiographic implications: Professional Paper, doi: 10.3133/pp252.

Malik, I., (2006), Contribution to understanding the historical evolution of meandering rivers using dendrochronological methods: example of the Mała Panew River in southern Poland: Earth Surface Processes and Landforms, v. 31, p. 1227–1245, doi: 10.1002/esp.1331.

Nanson, G.C., and Hickin, E.J., (1983), Channel Migration and Incision on the Beatton River: Journal of Hydraulic Engineering, v. 109, p. 327–337, doi: 10.1061/(asce)0733-9429(1983)109:3(327).

Pizzuto, J.E., and Mecklenburg, T.S., (1989), Evaluation of a linear bank erosion equation: Water Resources Research, v. 25, p. 1005–1013, doi: 10.1029/wr025i005p01005.

Pizzuto, J., (2009), An empirical model of event scale cohesive bank profile evolution: Earth Surface Processes and Landforms, v. 34, p. 1234–1244, doi: 10.1002/esp.1808.

Randle, T.J., (2004), Channel Migration Model for Meandering Rivers, p. 241–248.

Simon, A., Pollen-Bankhead, N., and Thomas, R.E., (2013), Development and Application of a Deterministic Bank Stability and Toe Erosion Model for Stream Restoration: Stream Restoration in Dynamic Fluvial Systems Geophysical Monograph Series, p. 453–474, doi: 10.1029/2010gm001006.

Appendix I: Annual Maximum Discharge data

			Decadal	Max
	Gage #	**Date**	**Q, cfs**	**Q, cfs**
USGS	1645000	7/1/1931	1730	
USGS	1645000	3/28/1932	1380	
USGS	1645000	8/24/1933		9300
USGS	1645000	9/17/1934	2410	
USGS	1645000	5/7/1935	1420	
USGS	1645000	1/3/1936	2020	
USGS	1645000	8/27/1937	2610	
		AVE	**1928**	
USGS	1645000	10/23/1937	2280	
USGS	1645000	1/30/1939	2150	
USGS	1645000	4/20/1940	1740	
USGS	1645000	6/23/1941	1300	
USGS	1645000	5/22/1942	1460	
USGS	1645000	10/16/1942		3620
USGS	1645000	11/9/1943	2660	
USGS	1645000	8/1/1945	2110	
USGS	1645000	6/2/1946	2940	
USGS	1645000	8/20/1947	1990	
USGS	1645000	6/30/1948	1990	
		AVE	2062	
USGS	1645000	7/16/1949	2240	
USGS	1645000	3/23/1950	2280	
USGS	1645000	12/4/1950	2420	
USGS	1645000	9/1/1952	2810	
USGS	1645000	11/22/1952	7330	
USGS	1645000	12/14/1953	1240	
USGS	1645000	8/13/1955	2620	
USGS	1645000	7/21/1956		15000
USGS	1645000	4/5/1957	959	
USGS	1645000	12/21/1957	3640	
		AVE	2838	
USGS	1645000	8/8/1959	1970	
USGS	1645000	2/19/1960	1600	
USGS	1645000	6/10/1961	3070	3070
USGS	1645000	3/12/1962	1920	

USGS	1645000	8/20/1963	1480	
USGS	1645000	1/9/1964	2520	
USGS	1645000	8/26/1965	2640	
USGS	1645000	9/14/1966		
USGS	1645000	8/27/1967	2660	
USGS	1645000	1/14/1968	1640	
		AVE	2167	
USGS	1645000	9/4/1969	3490	
USGS	1645000	7/10/1970	2200	
USGS	1645000	9/12/1971	25900	
USGS	1645000	6/22/1972		26100
USGS	1645000	9/14/1973	3020	
USGS	1645000	12/26/1973	3160	
USGS	1645000	9/26/1975	16000	
USGS	1645000	1/1/1976	4900	
USGS	1645000	10/9/1976	3770	
		AVE	7805	
USGS	1645000	1/26/1978	7850	
USGS	1645000	9/6/1979		16000
USGS	1645000	10/1/1979	10800	
USGS	1645000	2/11/1981	1340	
USGS	1645000	6/13/1982	3160	
USGS	1645000	4/10/1983	3260	
USGS	1645000	3/29/1984	3010	
USGS	1645000	2/12/1985	3620	
USGS	1645000	4/16/1986	1070	
USGS	1645000	9/9/1987	4950	
USGS	1645000	5/19/1988	7410	
			4647	
USGS	1645000	5/6/1989	8250	
USGS	1645000	4/2/1990	2270	
USGS	1645000	10/23/1990	5120	
USGS	1645000	3/27/1992	1750	
USGS	1645000	4/16/1993	3350	
USGS	1645000	11/28/1993	9160	
USGS	1645000	8/6/1995	2080	
USGS	1645000	6/18/1996		11000
USGS	1645000	10/19/1996	3880	

USGS	1645000	3/21/1998	5280	
		AVE	4571	
USGS	1645000	9/16/1999	3060	
USGS	1645000	3/22/2000	1910	
USGS	1645000	8/12/2001	3140	
USGS	1645000	5/27/2002	4310	
USGS	1645000	9/23/2003		7130
USGS	1645000	12/11/2003	6810	
USGS	1645000	7/8/2005	3750	
USGS	1645000	6/26/2006	6530	
USGS	1645000	11/17/2006	5790	
USGS	1645000	5/12/2008	3660	
		AVE	4329	
USGS	1645000	5/26/2009	2650	
USGS	1645000	12/26/2009	2930	
USGS	1645000	9/8/2011		24400
USGS	1645000	10/13/2011	2890	
USGS	1645000	1/31/2013	8280	
USGS	1645000	5/16/2014	7040	
USGS	1645000	6/28/2015	4950	
USGS	1645000	7/31/2016	3350	
USGS	1645000	7/29/2017	3490	
		AVE	**4448**	
	Decadal Discharge Summary			
	Decade	Qmean	Qmax	
	1935	1928	9300	
	1945	2062	3620	
	1955	2837	15000	
	1965	2166	3270	
	1975	7805	26100	
	1985	4647	16000	
	1995	4571	11000	
	2005	4328	7130	
	2015	4448	24400	

Appendix II: USGS gauging station data for 1949-1958

Channel Discharge	Channel Width	Channel Velocity	Channel Depth
238	55	3.42	1.267272727
211	53	3.13	1.271698113
237	56	3.44	1.244642857
155	72	2.75	0.783333333
112	47	2.06	1.157446809
112	48.5	2	1.156701031
106	47	1.97	1.144680851
62.8	52.5	1.5	0.794285714
73.5	46	1.53	1.045652174
54.8	50.5	1.51	0.720792079
43.3	46	1.16	0.813043478
343	65.5	3.36	1.557251908
73.8	45	1.6	1.035555556
85.9	47	1.8	1.014893617
92.2	49	1.71	1.1
89.2	52.5	1.52	1.12
133	64	2.51	0.828125
114	51.8	2.41	0.913127413
96.4	53	1.99	0.911320755
66.9	46.5	1.51	0.95483871
51.1	45	1.33	0.851111111
32.9	50	1.3	0.506
41.2	50	1.33	0.62
51.2	45	1.33	0.855555556
56.2	47	1.46	0.819148936
82.4	45.5	1.75	1.032967033
160	53.6	2.49	1.199626866
100	53	2.04	0.922641509
261	87	3.14	0.954022989
131	45	2.17	1.342222222
129	64	2.6	0.978125
163	70	2.73	0.854285714
70.2	53.5	1.87	0.702803738
216	68	2.78	1.141176471
71.9	49.5	1.45	1.004040404
34.7	42	0.89	0.928571429
26.8	46.5	0.89	0.64516129
28.9	44	0.74	0.886363636
48.2	50	1.1	0.87
244	54	2.74	1.646296296
75.8	47.5	1.32	1.208421053
50.2	54	1.25	0.744444444

45.5	48.5	0.4	1.039175258
144	47.5	2.17	1.4
501	47	1.09	1.170212766
56.8	52.5	1.75	0.619047619
46.7	46	1.21	0.841304348
41.8	49.5	0.83	1.022222222
42.9	47.5	0.87	1.035789474
242	68	3.21	1.108823529
81.6	53	2.14	0.720754717
136	52	1.89	1.380769231
321	55.5	2.89	2
503	72	3.75	1.861111111
106	47	1.67	1.35106383
1810	165	3.6	3.054545455
152	55	2	1.381818182
97.7	54.4	1.6	1.119485294
55.4	57.5	1.11	0.871304348
2680		2.21	
2310	540	2.14	2
60	53	1.42	0.794339623
53	46	1.19	0.97173913
7330			
107	66	2.11	0.783333333
114	54.5	1.45	1.44587156
115	51	1.57	1.435294118
158	54	1.8	1.622222222
60.1	53	1.26	0.9
43	53.5	0.86	0.940186916
27.9	27.5	1.43	0.709090909
42.5	41	1.08	0.96097561
65.3	42.5	1.4	1.101176471
80.3	42	1.62	1.178571429
41.4	53.5	1	0.771962617
13	19.6	1.09	0.607142857
10.2	20.5	0.91	0.546341463
27.5	30	1.16	0.79
25.8	26.2	1.07	0.923664122
59.8	45	1.2	1.104444444
22.3	26	1.18	0.726923077
8.19	23	0.65	0.547826087
34.9	34.5	1.63	0.620289855
34.7	34	1.48	0.688235294
47	35	1.71	0.785714286
29.4	28.5	1.3	0.792982456
107	68	2.06	0.764705882
94.4	51	1.57	1.178431373

47.4	34.5	1.72	0.8
60.4	44	1.38	0.997727273
103	41	2.38	1.056097561
61.7	33	1.88	0.996969697
179	60	2.48	1.201666667
75.7	54	1.53	0.918518519
28.6	28	1.3	0.842857143
13.7	38	1.75	0.062631579
16	47	0.47	0.744680851
15.9	25	0.89	0.72
174	65	2.44	1.107692308
88.2	49.5	1.68	1.060606061
67.9	33	1.55	1.324242424
26.4	72	2.69	1.359722222
83.6	50	1.61	1.036
133	54	2	1.231481481
56.2	53	1.53	0.69245283
45.8	51	0.91	0.982352941

* I pledge on my honor that I have not given or received any unauthorized assistance on this research.*